Available online at www.sciencedirect.com
SCIENCE DIRECT®
Polymer 44 (2003) 6589–6598
polymer
www.elsevier.com/locate/polymer

NMR and calorimetric investigation of water in a superabsorbing crosslinked network based on cellulose derivatives

D. Capitani[a]*, G. Mensitieri[b,]*, F. Porro[b], N. Proietti[a,c], A.L. Segre[a]

[a]*Institute of Chemical Methodologies, CNR, Research Area of Rome, M.B.10, 00016, Monterotondo Stazione, Rome, Italy*
[b]*Department of Materials and Production Engineering, University of Naples 'Federico II', P.le Tecchio 80, 80125 Naples, Italy*
[c]*CAMPEC, Via G. Porzio, Centro Direzionale, Isola F4, Naples, Italy*

Received 27 April 2003; received in revised form 25 July 2003; accepted 6 August 2003

Abstract

In this study we have investigated the state of water in a superabsorbing network based on hydroxyethylcellulose (HEC) and carboxymethylcellulose sodium salt (CMCNa) crosslinked with divinylsulfone (DVS).

This type of network, at low degree of crosslinking, when exposed to distilled water is able to form a stable hydrogel containing an amount of water as high as 1000 times its own weight.

De-hydrated/re-hydrated networks, containing different amounts of absorbed water, have been studied using differential scanning calorimetry (DSC) and NMR relaxometric methods. DSC analysis allowed the evaluation of freezable and non-freezable fractions of absorbed water showing also the presence of two types of freezable water. On the other hand, NMR relaxometry evidenced the presence of two hydration shells, characterized by a different mobility, which in both cases is lower than that of bulk water.

An excellent quantitative agreement was found in the determination of the amount of freezable water using the two techniques.

A comparison of the state of water in the crosslinked network and in the corresponding uncrosslinked mechanical mixture shows that in the last case micro-heterogeneity arises.

Keywords: NMR; Calorimetry; Superabsorbing hydrogel

1. Introduction

Superabsorbing networks based on cellulose derivatives can be synthesized with sorption properties similar to those displayed by acrylate based products [1,2]. These materials can be obtained by chemical crosslinking of cellulose polyelectrolyte derivatives using small difunctional molecules as crosslinkers, which form a three dimensional hydrophilic network through intermolecular covalent bonds among polymer molecules. Further improvement of water sorption capacity can be obtained by inducing the formation of a microporous structure [2]. These crosslinked materials are able of absorbing an amount of water even higher than 1000 times their own weight.

A ^{13}C solid state NMR analysis was previously performed [3] on dry microporous networks based on hydroxyethylcellulose (HEC) and sodium salt of carboxymethylcellulose (CMCNa) crosslinked with divinylsulfone (DVS). Degrees of crosslinking of different networks were determined using solid state NMR, free swelling in water and uniaxial compression of water swollen samples [4]. A good agreement among the three approaches has been found in terms of concentration of crosslinks per unit volume of dry polymer. The results have been discussed taking into account that NMR technique is able to detect only chemically effective crosslinks, while free swelling and compression are sensitive to elastically effective physical and chemical crosslinks [4].

Besides the degree of crosslinking, another important issue, which affects the swelling properties and performances of an hydrophilic polymeric network in an aqueous medium, is the behaviour of the water hosted into the polymeric material. Water embedded into polymeric

* Corresponding authors. Tel.: +39-81-768-2512; fax: +39-81-768-2404.
E-mail addresses: mensitie@unina.it (G. Mensitieri), capitani@imc.cnr.it (D. Capitani), fporro@unina.it (F. Porro), noemi.proietti@imc.cnr.it (N. Proietti), segre@imc.cnr.it (A.L. Segre).

0032-3861/$ - see front matter © 2003 Elsevier Ltd. All rights reserved.
doi:10.1016/j.polymer.2003.08.007

matrices behaves anomalously in the sense that the first order transitions which characterize pure bulk water are modified; for instance the freezing temperature of confined water is lowered. Many factors complicate the interpretation of data from hydrated polymers [5]. In fact, depending both on the temperature and concentration, water may act as plasticizer or anti-plasticizer. Moreover, hydration and crosslinking may induce significant conformational changes in the polymeric matrix while mobility of the network affects the organization of the confined water [6].

As many as four distinguishably different types of water, ranging from the very tightly bound to free, bulk-like water have been reported in the literature [7]. Experimental methods, based on DSC and NMR measurements aimed to get an estimate of the amount of *freezable water*, are described in the literature [8,9]. Calorimetric methods, such as differential scanning calorimetry (DSC), have been used to monitor the gross phase changes of water in polymeric networks. Such thermodynamic measurements allow the characterization of hydrated systems without the need of detailed molecular models. Pulsed low resolution NMR is an important tool allowing an insight into the dynamic of water molecules and their environment. Recently [10], we applied low resolution NMR to explain the experimental observation that lightly crosslinked chitosan chains can absorb water in amounts higher than those observed in the case of their parent polymer. We observed water in different solvation states and obtained a quantitative evaluation of water in different shells.

In this study, we analyse the state of water molecules confined in CMCNa/HEC/DVS superabsorbing networks as compared to the case of uncrosslinked CMCNa/HEC mixture. Complementary information on the dynamics of water molecules and on the thermophysical macroscopic behaviour is gathered, respectively, from low resolution NMR and from DSC. A quantitative evaluation of water belonging to the first solvation shell is also performed.

2. Experimental section

2.1. Materials

CMCNa (cod 41,933-8), HEC (cod. 30,683-3) and DVS (cod. V370-0) were purchased from Aldrich Chimica s.r.l. Milano and used as received.

2.2. Sample preparation

Crosslinking reaction was performed according to procedures reported in the literature [1]. A mixture of CMCNa and HEC, with a weight ratio equal to 3/1, was dissolved in a solution of DVS and distilled water by gently stirring at room temperature until a transparent solution was obtained. The adopted polymer weight fraction in the solution was 2%; the concentration of DVS was 0.133 mol per liter of solution. After stirring, an aqueous solution of KOH (1 M) was added to catalyze the polymer solution. In a few hours, a partially swollen hydrogel was obtained. To remove unreacted DVS and KOH, the obtained hydrogel was cut in small pieces and then soaked several times in fresh distilled water under continuous stirring. The degree of crosslinking, as measured via NMR and free swelling in distilled water, was around 8 mol of crosslinks per cm^3 of dry network [4]. The purified hydrogel was then desiccated at atmospheric pressure, room temperature and 50% relative humidity. This desiccation process typically took as long as 1 week. As calculated from thermo-gravimetric measurements, the amount of residual water still contained in the hydrogel after this stage was about 10% by weight. To further proceed with desiccation, samples were finely grinded and kept several days under vacuum (10^{-3} Torr) at 40 °C until a constant weight was attained.

Uncrosslinked samples were also prepared. To this aim an aqueous solution of CMCNa, HEC was prepared with an overall polymer concentration of 2% by weight and with a CMCNa/HEC ratio equal to 3/1. The desiccation and grinding stages were carried out as for the crosslinked samples.

2.3. Sample re-hydration

After desiccation, the powder of crosslinked (C) and uncrosslinked (U) CMCNa/HEC samples was re-hydrated under well controlled temperature and humidity conditions. To this aim, powder samples were placed in a water jacketed vacuum tight container, kept at 25 °C, connected to a distilled water container maintained at a lower controlled temperature. Different humidity could be realized in the sample chamber by changing the temperature of the water reservoir. Before re-hydration the sample container was evacuated through service lines connected to a turbo-molecular pump.

Samples for the NMR analysis were initially placed in NMR tubes and then in the container. Vacuum was applied and then the container was connected to the water reservoir at the requested temperature. After the necessary time to attain the sorption equilibrium (previous sorption experiments were performed to determine sorption kinetics), the sample container was opened, NMR tubes rapidly removed and sealed using a Bunsen flame.

In the case of DSC samples, the powder was introduced in the sample container already in the DSC aluminium pans, which were opened to insure the contact with the humid atmosphere. After the attainment of equilibrium, pans were quickly removed, hermetically closed and placed in the DSC instrument.

The amount of water absorbed in the samples was determined by weighing aluminium containers where few grams of powder were placed, which were exposed to the same humid environment as for the samples to be used for NMR and DSC measurements. After the proper lapse of

time the aluminium containers were removed from the apparatus, closed and weighted. In this way, the sorbed amounts at equilibrium and the associated kinetics were determined. In the following we will report the amount of sorbed water in the samples as $W_0 =$ [mol of added water]/[mol of the polymer repeating unit]. The molecular weight of average repetitive unit has been evaluated [4] to be 200 g/mol.

The procedure described above was used in the case of a small amount of sorbed water. For greater amounts ($W_0 >$ 30), desiccated powder was placed in a glass vial, the right amount of water added by a micro-syringe and the vial sealed. After enough time was elapsed for the system to equilibrate, hydrated powder was then quickly removed from vials and sealed in NMR tubes or DSC pans.

In order to confirm the amount of added water, thermogravimetric analysis was also performed on samples prepared with the above procedure.

2.4. DSC measurements

DSC tests were carried out on several samples characterized by a different amount of sorbed water. Samples with $W_0 = 0$, 4.5, 11.2, 27.3, 41.5, 62.2, 91.2, 136.9 and 182.5 were prepared. Powder samples, with a typical weight of 10 mg, were placed in hermetically sealable aluminium pans for liquids. Tests were run using a TA Instrument mod. 2920 equipped with a liquid nitrogen automatic cooling system.

Phase transitions of water were investigated by first quickly cooling the sample down to -70 °C, equilibrating for 10 min at this temperature and then heating at a rate of 5 °C/min up to 30 °C. As reported in literature [8], the adopted heating rate guarantees a good quality of calorimetric response associated to the physical phenomena occurring during the scan. The results of this analysis should be, in principle, the same as those obtainable by imposing a cooling scan from 30 to -70 °C. As a matter of fact, this is not the case [11] likely due to evaporation and condensation processes inside the pan and to the dependence of the shape of water melting and crystallization peaks on heating − cooling cycles. On the basis of these considerations and in view of the better performances of the instrument when working in the heating mode, we decided to perform the DSC analysis only by imposing single heating ramps.

Area of peaks and onset temperatures of melting have been calculated automatically using the post-analysis software of the instrument.

2.5. NMR relaxation measurements

(C) and (U) powders with $W_0 = 0$, 0.8, 5.5, 10.9, 20.2, 30.0, 50.0, 70.0 and 100.0 and $W_0 = 5.3$, 10.2, 19.9, 30.0, 50.0, 70.0 and 100.0, respectively, were prepared. The powder samples were placed in standard 5 mm NMR tubes and sealed. In order to keep samples well within the NMR coil, the height of each sample was 0.4 cm.

Pulsed low resolution ^{1}H NMR measurements were performed at 75 MHz on a Spinmaster spectrometer, Stelar, Mede (Pavia), Italy. A variable temperature unit (Stelar, VTC91) was used in the temperature range 180–300 K. The dead time of the instrument is 7 μs. A variable attenuator placed between the transmitter output and the probe head, allowed to tune 90 and 180° pulses at 4 and 8 μs, respectively.

2.5.1. Free induction decay (FID)

FIDs were measured using the 90° pulse and a recycle delay of 10 s; 2048 or 4096 data points were collected in each experiment. The number of scans was optimized to obtain a good signal to noise ratio.

2.5.2. Spin-lattice relaxation times

T_1 spin-lattice relaxation times were measured with the Aperiodic Saturation Recovery [12,13] sequence. This sequence consists of 15 90° pulses. At the end of the pulse train the relaxation recovery proceeds with a variable delay τ_i placed before a fixed 90° pulse. The aperiodic saturation recovery sequence was run according to a multiblock, multiscan procedure; 128 data blocks, corresponding to 128 delays τ_i were collected in each experiment; each block was acquired with a size of 512 data points.

T_2 spin–spin relaxation time measurements (on the water component) were carried out using both the CPMG [14] and the AP-CPMG [15] sequence; the echo time was always kept at 100 μs. Depending on the T_2 length, 1024, 2048 or 4096 echoes were collected.

Errors due to chemical exchange, diffusion and spin–spin coupling are reduced or eliminated from T_2 measurements using the CPMG sequence. However, it has been previously shown [10,15] that in a very short 2τ regime, spins may not de-phase significantly in the time between pulses. As a result, spins may be locked by the effective refocusing field of the CPMG sequence which will measure the spin-lattice relaxation time in the rotating frame $T_{1\rho}$ instead of measuring the effective T_2.

In systems such as tissues, gels and viscous liquid [16,17], when $T_2 \ll T_{1\rho}$ spin-locking effects may affect the CPMG sequence leading to a marked increase in the measured spin–spin relaxation time.

In such a case, T_2 measured with the CPMG sequence in the short 2τ regime may be indistinguishable from $T_{1\rho}$ measured in a locking field equivalent to that one produced by the refocusing pulses.

As reported in the literature [15], the spin-locking effects can be eliminated using an alternating phase CPMG, namely the AP-CPMG sequence. In the measurements reported here, CPMG and AP-CPMG sequences give the same values for any echo time $2\tau \geq 80$ μs.

2.6. NMR data analysis

Analysis of NMR data was performed using the program 'Stefit' [18] that uses a 'Simplex' algorithm [19] for the fit of various functional forms.

2.6.1. FIDs

The shape of the FIDS has been fit to a sum of Gaussian line shapes [5]:

$$Y = C_0 + \sum_i W_i \exp\left[\frac{-t^2}{G_i^2}\right] \quad i = \text{number of Gaussian components}$$

being C_0 the mean value of the noise, W_i is the spin density of the i component and G_i is the width of the i Gaussian component. Second moments are calculated as in Ref. [10].

2.6.2. T_2 relaxation times

CPMG and AP-CPMG experiments lead to exponential or multiexponential decays:

$$Y = C_0 + \sum_i W_i \exp\left[\frac{-t}{T_{2i}}\right] \quad i = \text{number of components}$$

where C_0 is the mean value of the noise, W_i is the spin density of the i component and T_{2i} is the spin–spin relaxation time of the i component.

Note that T_2 is a monotonic function of the correlation time, thus the shorter is the T_2 value, the stiffer is the system.

2.6.3. T_1 relaxation times

In crosslinked networks with added water, due to different T_2 relaxation times, at least two Gaussian functions have been used for obtaining the FID shape. In an APSR multiblock experiment, each experiment leads to a FID obtained with the proper time increment τ_i, with $i = 1, \ldots, N$ and N = number of blocks. As shown in Fig. 1, at least two

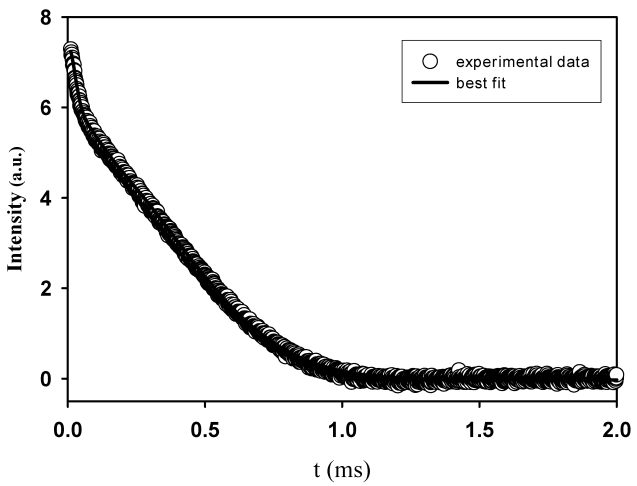

Fig. 1. Free induction decay (FID) of CMC/HEC/DVS network with $W_0 = 5.5$. The solid line through experimental points is obtained by applying a best fit procedure.

Gaussian components are observed in each FID of an APSR experiment. We label as 'A' the fast T_2 relaxing component and 'B' the slow T_2 relaxing component.

According to a previously published procedure [10], we cut each FID after a suitable initial delay. In this way we obtain T_1 value of the long T_2 relaxing component, T_{1B}, according to the equation:

$$I_{B_i} = B_0 + \exp(-\tau_i/T_{1B})$$

For obtaining the T_1 value of the short T_2 relaxing component, T_{1A}, a full best fit procedure of all N different FIDs must be applied.

2.6.4. Confidence intervals and errors

The best fit functions for FIDs, and T_1 and T_2 exponential decays have all been accepted with a confidence better than 95%.

Estimated errors are better than 5% of the nominal value for G_i and T_{2i} and better than 10% of the nominal value for T_{1i} and for all spin densities W_i. For second moments estimated errors are of the order of 20% of the nominal value.

2.6.5. Distribution of multiexponential functions

The visualization of multiexponential data, such as encountered T_2 decays, is often quite difficult. For each component it is necessary to compare the intensity, the value and the distribution. A possible way of performing any comparison is to perform an inversion of the data [20]. A basic equation describing the relaxation of magnetization in an NMR experiment is

$$y(t_i) = y_i = \int_{T_{\min}}^{T_{\max}} W(T)\exp(-t_i/T)\mathrm{d}T$$

In a discrete form a set of relaxation data y_i at times t_i equally spaced in $q_i = \ln t_i$ can be approximated with a sum of M exponential components:

$$y_i \cong W_0 + \sum_{k=1}^{M} W_k \exp\left(\frac{-t_i}{T_k}\right)$$

where W_k is the distribution of amplitudes at relaxation times T_k and W_0 is the signal amplitude at infinite time. For smoothing the data a penalty function is added to the squared root of fit [21], thus the function to minimize is:

$$\sum_{i=1}^{N}\left[W_0 + \sum_{K=1}^{M} W_k \exp\left(\frac{-t_i}{T_k}\right) - y_i\right]^2 + c_1 \sum_{k=1}^{M} W_k^2 + c_2 \sum_{k=1}^{M-1} \times (W_{k+1} - W_k)^2 + c_3 \sum_{k=2}^{M-1} (W_{k-1} - 2W_k + W_{k+1})^2$$

The best fit function has been implemented within a Matlab framework [22].

In the resulting distribution, the positions are the

relaxation time values while the areas correspond to the normalized spin densities.

3. Results and discussion

3.1. DSC analysis

Heating scans for samples containing different amounts of sorbed water are reported in Fig. 2. From the calorimetric traces it can be observed that the endothermic melting peak is present only for samples with W_0 greater than 4.5. The amount of *non-freezable water*, defined as the maximum amount of water present in the polymer which is not associated with any endothermic peak [8], has been evaluated as the intercept on the x axis of a linear fit of melting heat data reported as function of water content. This procedure, illustrated in Fig. 3, gives an amount of non-freezable water equal to 5.8 mol of water/moles of repeating unit.

It is worth noting that this procedure is based on two relevant hypotheses, the first being that the result obtained is not affected by the heat associated to water–polymer mixing which occurs right after melting and the second being that the amount of non-freezable water does not depend on the total amount of sorbed water. As reported in the literature [23] the first assumption is reasonable. The second one, however, is questionable, since it implies that the number of water molecules in the first shell of solvation, identified here with the non-freezable water, does not change varying the polymer–water molar ratio and the

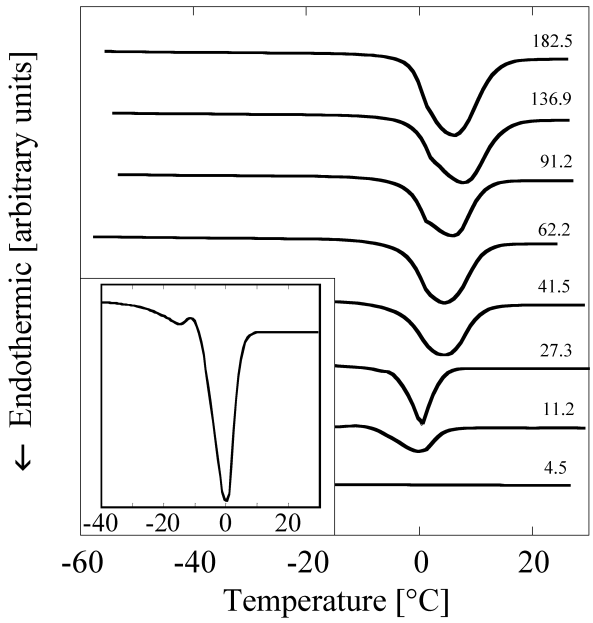

Fig. 2. DSC scans for hydrogel samples with different water content. Labels on curves represent the amount of water as W_0 = [moles of added water]/[moles of polymer repeating units]. In the inset is reported the detail of water melting peak for a sample with $W_0 = 11.2$.

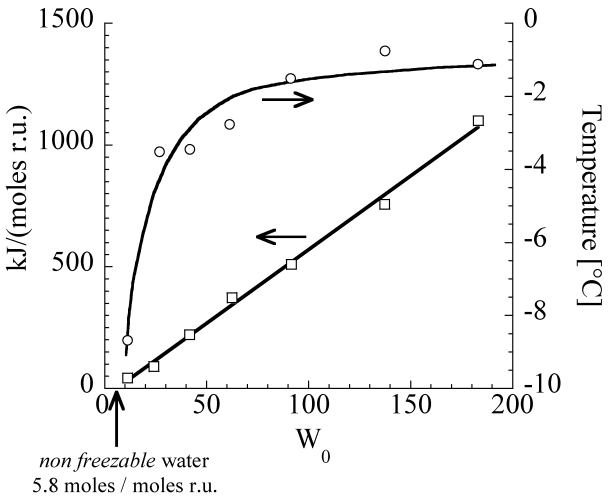

Fig. 3. Heat of melting of water added to the hydrogel (line represents linear fitting) and onset temperature of melting of freezable water (line drawn to guide the eye) reported as function of W_0.

temperature. This hypothesis is consistent only if a monotonous trend is observed for the NMR transversal relaxation time as a function of the temperature at each water–polymer molar ratio. Indeed this observation holds in the case of CMC/HEC, while, for instance, it is not true in the case of chitosan based networks [10].

Onset temperature of water melting is affected by the amount of sorbed water. In fact, melting temperature steadily increases with the amount of added water and approaches asymptotically the melting temperature of bulk water, see Fig. 3. The reported dependence is alike to that of the melting temperature of water placed inside capillary holes on the radius of the capillary itself [24]. On this basis, the observed increase of the onset temperature can be attributed to the corresponding increase of average dimension of channels where freezing water is located.

It is worth of note that samples containing a small amount of freezable water display a DSC trace characterized by a double melting peak. The case of a sample characterized by $W_0 = 11.2$ is reported in the inset of Fig. 2. This phenomenon can be tentatively attributed to the existence of two types of freezable water: water melting at lower temperature, often reported as freezable bound water, and water melting at higher temperature, reported simply as freezable water [25]. As the amount of sorbed water increases, the two peaks merge to form a single broad peak characterized by the presence of a small shoulder at low temperature.

3.2. NMR data

3.2.1. FID measurements

In order to study the water–polymer interaction, a careful NMR study was performed on partially re-hydrated samples with different amount of added water.

When no water is added ($W_0 = 0$), in the full range of

temperatures, only one Gaussian component is observed. In all other samples with $W_0 > 0$, the analysis of the FIDs shows the presence of at least two Gaussian components, see Fig. 1.

In Fig. 4, the spin densities W_a and W_b are reported vs the temperature. W_a is the spin density of the fast decaying component. According to the literature this component is due to the macromolecule with its exchangeable hydroxyl groups and possibly to water very tightly bound to the macromolecule itself by hydrogen bonds. W_b is the spin density of the slow decaying component which is due to water in other shells of solvation.

With regard to the rigid, fast decaying component of the FID, a net increase of its spin density is observed when a fraction of the gel freezes. This effect is observed near the melting point of a confined solvent in the presence of its free state. At about 265 K, a net decrease of W_b along with a net increase of the corresponding W_a is observed in samples with $W_0 \geq 10.9$. At about 200 K $W_b \cong 0$ and $W_a \cong 1$, i.e. all bound water is frozen. In samples with $W_0 \leq 5.5$, as a function of the temperature, W_a and W_b both show a rather continuous trend. A possible interpretation of these data is that the polysaccharide is able to tightly coordinate an amount of water molecules for repeating unit ranging between 6 and 9. This value is in close agreement with the amount of freezable water detected by DSC measurements, i.e. 5.8 water molecules for repeating unit.

Data on the second moments M_a and M_b vs temperature are reported in Fig. 5 for samples with $W_0 = 0$, 0.85, 5.5,

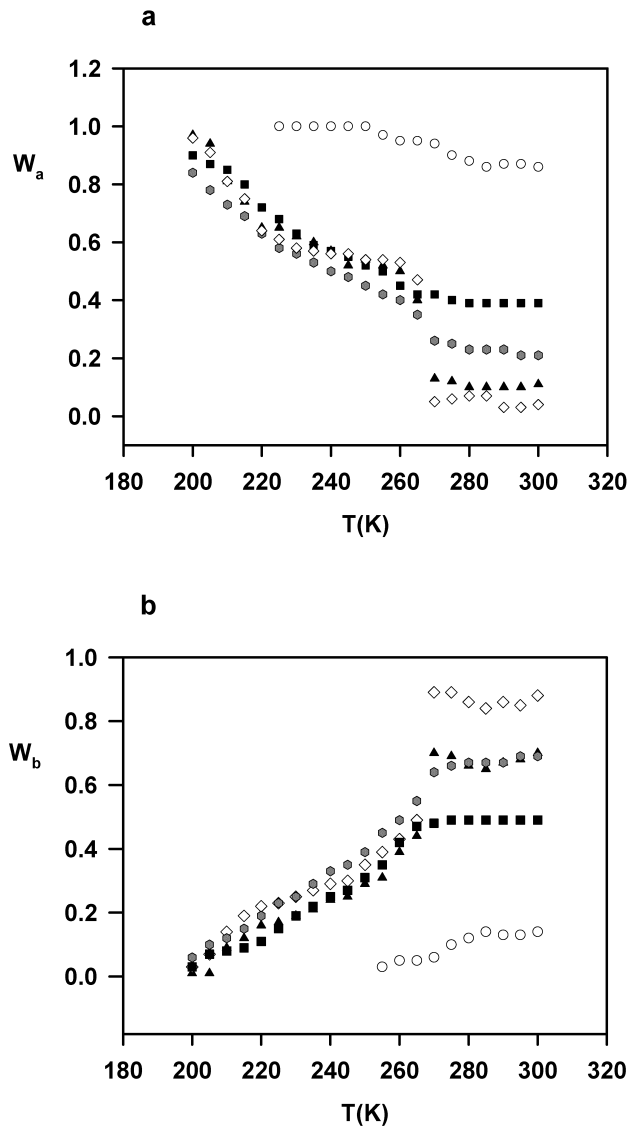

Fig. 4. Normalized spin density of the fast (a) and slow (b) decaying components of the FID as a function of the temperature. $W_0 = 0.8$ (○); $W_0 = 5.5$ (■); $W_0 = 10.9$ (⬢); $W_0 = 20.2$ (▲); $W_0 = 30.0$ (◇).

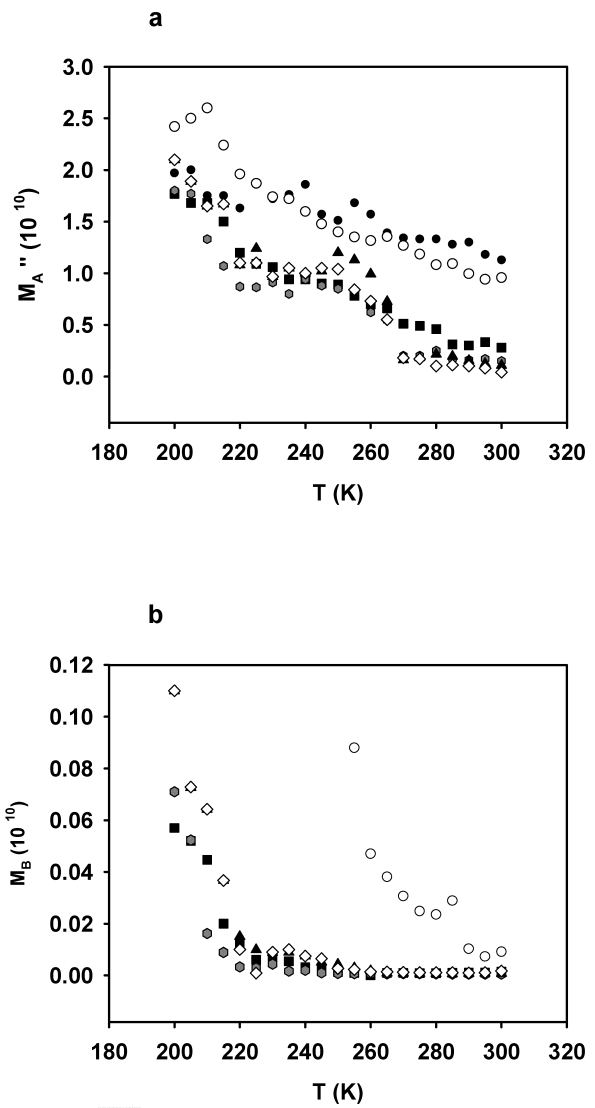

Fig. 5. Second moments M_a (a) and M_b (b) obtained from the FID reported vs temperature. $W_0 = 0$ (●); $W_0 = 0.8$ (○); $W_0 = 5.5$ (■); $W_0 = 10.9$ (⬢); $W_0 = 20.2$ (▲); $W_0 = 30.0$ (◇).

10.9, 20 and 30. It is worth of note the different behavior of M_b at $W_0 = 0.8$ with respect to the one shown at $W_0 > 0.8$. Note also that in samples with $W_0 > 0.8$ all M_b values are about the same. A possible explanation is that at $W_0 = 0.8$, since the water content is rather low, the exchange process is not very effective, while at $W_0 \geq 5.5$ it becomes the dominant process. Note that M_b values of samples with W_0 ranging from 5.5 up to 30 are very close to each other. Possibly due to the very fast exchange among shells, a clear classification of shells of solvation higher than the first one, is unpaired.

3.2.2. T_1 spin-lattice relaxation times

T_1 measurements can be separately performed on the fast T_2 decaying signal due to the polysaccharide and on to the slow T_2 decaying signal due to the water. It is possible to measure the relaxation time of the polysaccharide, T_{1p}, using the first few points of the magnetization measured in the time domain corresponding to the 8–20 μs range. Conversely, using points after at least 80 μs we obtain the relaxation time of the water component T_{1w}. Further details are given in the experimental section. Plotting T_{1p} vs T_{1w} values measured in the 200–300 K range of temperature, see Fig. 6, a straight line is obtained with an almost perfect coincidence with the $y = x$ line; in the full investigated range of temperature T_{1p} and T_{1w} values are the same within the experimental error. This identity is due to a strong spin-diffusion operating from the polysaccharide matrix to the water. Thus, even in the presence of marked difference in the line width and, consequently in T_2 values, T_1 values are indistinguishable.

In Fig. 7 are reported the spin-lattice relaxation times of samples with different values of W_0 as a function of 1000/T. It is worth noting that samples with $W_0 \geq 5.5$ show a flat, well defined minimum which is fully absent in the dry polymer and in sample with low water content. At temperatures lower than 220 K and $W_0 \geq 5.5$, log T_1 is linearly dependent on 1000/T. From the slope of the curve the activation energy for the overall motions of the polysaccharide–water (ice) system can be easily obtained, which is about 27 kJ/mol [5].

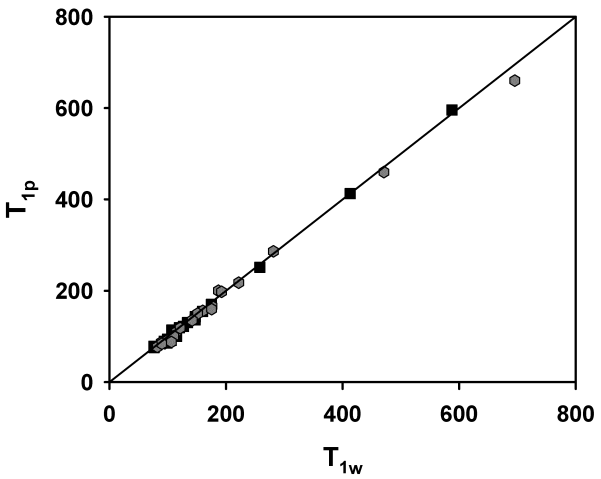

Fig. 6. T_1 spin-lattice relaxation time of the polysaccharide T_{1p}, vs the corresponding T_{1w} of the water, in the 200–300 K temperature range. The solid line through experimental points is obtained applying a linear regression procedure. $W_0 = 5.5$ (■); $W_0 = 10.9$ (⬢).

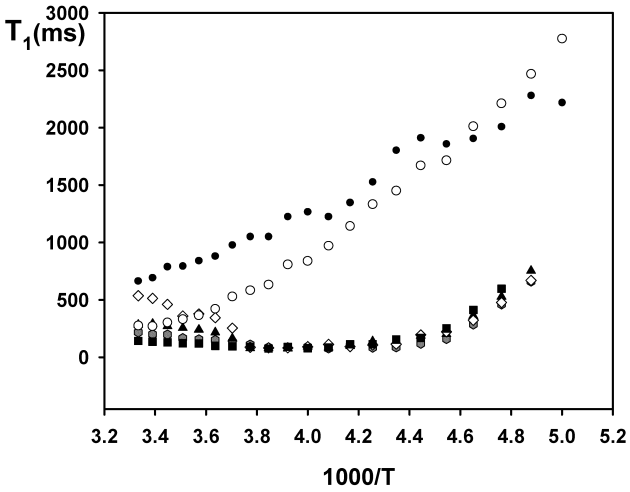

Fig. 7. T_1 spin lattice relaxation time vs 1000/T. $W_0 = 0$ (●); $W_0 = 0.8$ (○); $W_0 = 5.5$ (■); $W_0 = 10.9$ (⬢); $W_0 = 20.0$ (▲); $W_0 = 30.0$ (◇).

3.2.3. T_2 spin–spin relaxation measurements

It must be pointed out that a T_2 measurement can be performed with an echo train only on rather sharp lines. Thus, when we perform a T_2 measurement on a system such as a re-hydrated hydrogel, the measurement will be relevant for the water component while, the component relative to the macromolecule will disappear.

In all crosslinked samples, the echo train obtained applying the CPMG sequence fits with a single exponential decay. As a consequence, in the investigated range of temperature, a single T_2 value is obtained, see Fig. 8. In samples with $W_0 \geq 5.5$ T_2 undergoes a transition through 265 K; the gradient of T_2 becomes steeper with increasing the water content. Thus, on average, about 7–8 water molecules are tightly bound to the crosslinked network. As the water content increases, an increase in the amount of free or nearly free water is observed.

In the case reported here, all solvation shells, but the first one including the very tightly bound water, are in a very fast exchange, with water molecules continuously jumping from one solvation shell to another one.

3.2.4. T_2 distributions obtained applying inversion functions

The overall dependence of T_2 on the water content usually deals with the notion of heterogeneous water sites in the sense of different environments or, indeed, different averages for a given environment. Hence, even in the presence of just one single exponential decay, the obtained relaxation time may be represented as a distribution. From

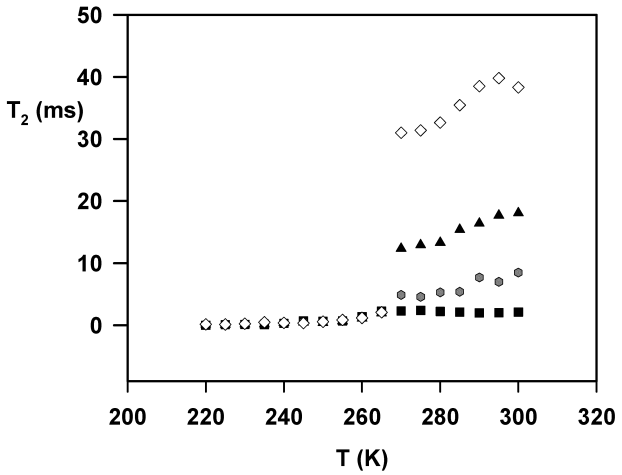

Fig. 8. T_2 spin–spin relaxation times vs temperature. $W_0 = 5.5$ (■); $W_0 = 10.9$ (⬢); $W_0 = 20.2$ (▲); $W_0 = 30.0$ (◇).

the decay curves obtained with a CPMG sequence, the corresponding distributions may be evaluated. The obtained distribution will be centered at a given position corresponding to the relaxation time and with an area corresponding to the signal amplitude. In this way a quick and easy representation of relaxation data may be obtained.

In Fig. 9, the distributions of T_2 relaxation data for samples with $W_0 = 5.5(a)$, 10.9 (b), 20.2 (c) and 30.0 (d) are given as a function of the temperature.

3.2.5. Comparison between crosslinked and uncrosslinked samples

Both crosslinked and un-crosslinked CMC/HEC mixtures are able of absorbing water, however, the un-crosslinked mixture is not a super-absorbing system. In fact, due to the linear structure of macromolecules and their ability to develop inter and intra-molecular hydrogen bonding, CMC and HEC polymer chains tend to densify. Therefore, in spite of the intrinsic hydrophilicity of these cellulosic chains, their interaction with water molecules is

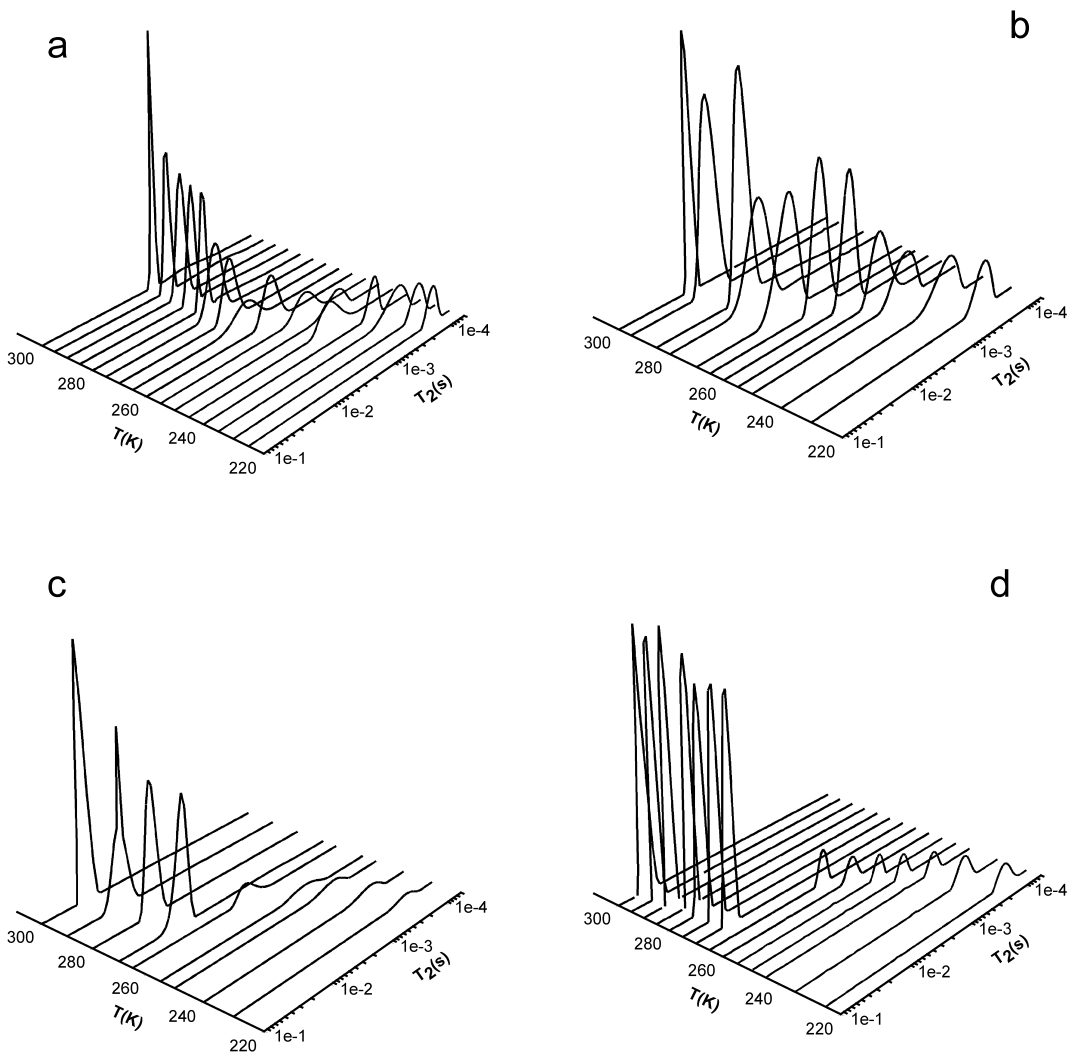

Fig. 9. Distribution of T_2 relaxation data as a function of the temperature at (a) $W_0 = 5.5$; (b) $W_0 = 10.9$; (c) $W_0 = 20$; (d) $W_0 = 30$.

largely reduced, at least as far as kinetics is concerned. Furthermore, as can be easily detected experimentally, water absorbed in the un-crosslinked material is readily released under mild compressive stresses, while in the same conditions the crosslinked material retains quite all the absorbed water. In the un-crosslinked samples, for concentrations exceeding a minimum value, water molecules are likely to collect in small gaps among the polymer chains, giving rise to heterogeneity in the material. This is also suggested by the results of the NMR analysis reported below. On the other hand, the presence of DVS in the crosslinked material is likely to hamper compaction of macromolecules and thus kinetically favors the interaction of water molecules with hydrophilic moieties and the homogeneous distribution of water molecules in the network, preventing also polymer dissolution.

To gather information on polymer–water interaction a careful T_2 study was performed at 300 K comparing data obtained on crosslinked samples with $W_0 = 5.5$, 10.9, 20.2, 30.0, 50.0, 70.0, 100.0, with data obtained with the uncrosslinked samples with amounts of added water, i.e. $W_0 = 5.3$, 10.2, 19.9, 30.0, 50.0, 70.0, 100.0.

Again, applying an inversion function to relaxation decays, a quick and easily readable information is obtained, see Fig. 10a and b. In Fig. 10a are shown T_2 distributions obtained for crosslinked samples at room temperature as a function of the water content: note that even at very high content of added water, a single sharp T_2 component is obtained. As expected, the value T_2 increases by increasing the water content. In Fig. 10b, the corresponding data are given at different W_0 for the mechanical uncrosslinked mixture are shown. In this mechanical mixture the most relevant point is that, starting from $W_0 = 20$ up to $W_0 = 100$, a bi-exponential decay is observed, corresponding to two T_2 distributions. The second component accounts for about 10% of the total amount of water. This observation points to the existence of at least two phases in the uncrosslinked samples, or, in other words, un-crosslinked samples start to exhibit micro-heterogeneity at $W_0 \geq 20$.

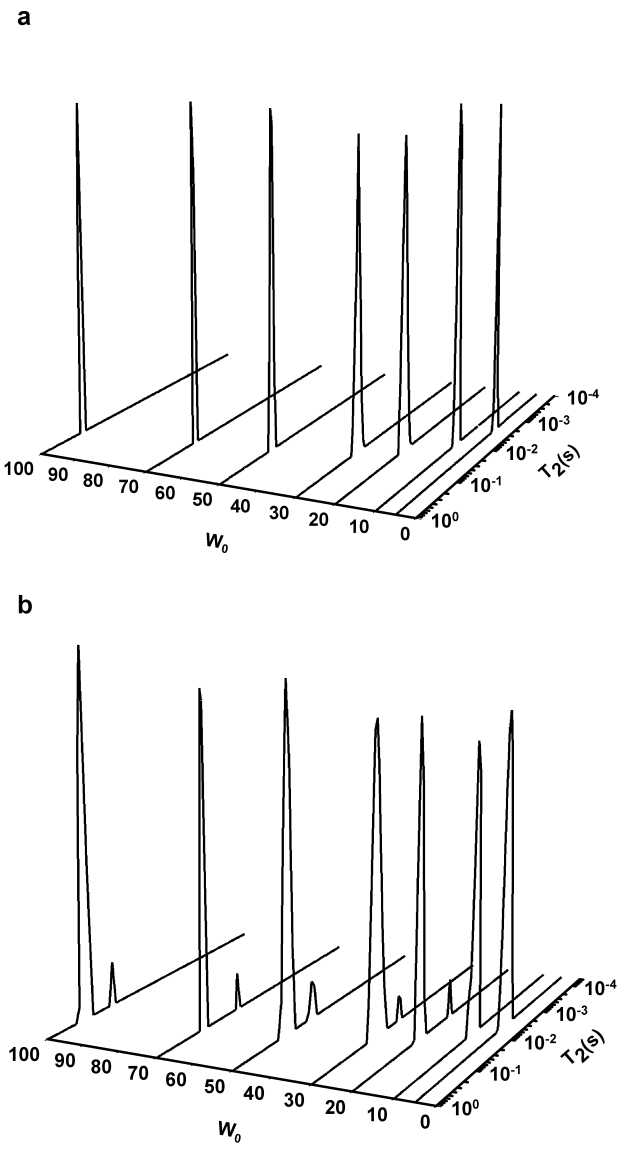

Fig. 10. Distribution of T_2 relaxation data at $T = 300$ K, (a) crosslinked sample at different W_0, $W_0 = 5.5$, 10.9, 20.2, 30.0, 50.0, 70.0, 100.0; (b) uncrosslinked sample at different W_0, $W_0 = 5.3$, 10.2, 19.9, 30.0, 50.0, 70.0, 100.0.

4. Conclusion

The state of water in a cellulose based super absorbing polymer crosslinked by DVS has been investigated by using NMR relaxometry and DSC analysis. For the sake of comparison, the NMR analysis has been also performed on the corresponding uncrosslinked polymer.

Two kinds of water, coexisting in the polymer, have been evidenced: non-freezable (or bound) water and freezable (or free) water.

Non freezable water is unable to solidify and is located in close proximity of the polymer backbones. Its mobility is lowered by the presence of dipolar interactions (hydrogen bonds) with macromolecules and by the peculiar microstructure of the material.

Freezable water forms the more external hydration shell of the macromolecules, it is able to solidify and is characterized by a higher mobility.

In agreement with current literature [8,9] the chemical interpretation of DSC data is based on two relevant hypotheses: the first being that the result obtained is not affected by the heat associated to water–polymer mixing which occurs right after melting and the second being that the amount of non-freezable water does not depend on the total amount of sorbed water. The first assumption is reasonable, as reported in literature [23], while the second one can be safely adopted for the case at hand since a monotonous trend is observed for the NMR transversal relaxation time as a function of the temperature at each water–polymer molar ratio. Actually, DSC analysis

evidenced the presence of two types of freezable water while NMR relaxometry evidenced the presence of two hydration shells, one more rigid and the other less rigid, even though his mobility is still lower than that of bulk water.

Using the NMR and DSC techniques it was possible to quantify the amount of each type of water with an excellent quantitative agreement between the two experimental approaches.

Distributions of T_2 spin–spin relaxation times measured on water allowed to promptly evidence heterogeneity in the case of the uncrosslinked mixture, while crosslinked network retains its homogeneity even at very high water content.

Acknowledgements

Thanks are due to R. Lamanna for performing the inversion of relaxation data.

References

[1] Anbergen U, Oppermann W. Polymer 1990;31:1854–8.
[2] Esposito F, Del Nobile MA, Mensitieri G, Nicolais L. J Appl Polym Sci 1996;60:2403–7.
[3] Capitani D, Del Nobile MA, Mensitieri G, Sannino A, Segre AL. Macromolecules 2000;33(2):430–7.
[4] Lenzi F, Sannino A, Borriello A, Porro F, Capitani D, Mensitieri G. Polymer 2003;44:1577–88.
[5] McBrierty VJ, Packer KJ. Nuclear magnetic resonance in solid polymers. Cambridge: Cambridge University press; 1993.
[6] Segre AL, Proietti N, Seta B, Daprano A, Amato ME. J Phys Chem B 1998;102:10248–54.
[7] Haly AR, Snaith JW. Biopolymers 1971;10:1681–99.
[8] Quinn FX, Kampff E, Snyth G, McBrierty V. Macromolecules 1988; 21:3191–8.
[9] Smyth G, Quinn FX, McBrierty V. Macromolecules 1988;21: 3198–204.
[10] Capitani D, Crescenzi V, De Angelis AA, Segre AL. Macromolecules 2001;34:4136–44.
[11] Mansor BA, Malcolm BH. Polym Int 1994;33:273–7.
[12] Fukushima E, Roeder SBW. Experimental pulse NMR. A nuts and bolts approach. Reading, MA: Addison-Wesley; 1981.
[13] Capitani D, Segre AL, Pentimalli M, Ragni P, Ferrando A, Castellani L, Blicharski JS. Macromolecules 1998;31:3088–93.
[14] Meiboom S, Gill D. Rev Sci Instrum 1958;29:688–91.
[15] Suh BJ, Borsa F, Torgeson DR. J Magn Reson 1994;A110:58–61.
[16] Santyr GE, Henkelman M, Bronskill MJ. J Magn Reson 1988;79: 28–44.
[17] Kurland RJ, Ngo FQH. J Magn Reson 1986;73:425–31.
[18] Sykora, S. *Program STEFIT*, part of Spinmaster software.
[19] Press WH, Teukolsky SA, Flannery BP, Vetterling WT, editors. Numerical recipes. The art of scientific computing. Cambridge: Cambridge University Press; 1988.
[20] Whittall KP, Bronskill MJ, Henkelman RM. J Magn Reson 1991;95: 221–34.
[21] Borgia GC, Brown RJS, Fantazzini P. J Magn Reson 1998;132: 65–77.
[22] Lamanna, R, personal communication.
[23] Bowstra JA, Salomons-de Vries MA, van Miltenburg JC. Thermochim Acta 1995;248:319–27.
[24] Skapski A, Billups R, Rooney A. J Chem Phys 1957;26:1350–1.
[25] Ping ZH, Nguyen QT, Chen SM, Zhou JQ, Ding YD. Polymer 2001; 42:8461–7.